

## THE SUPERCONDUCTING 130 MeV ELECTRON ACCELERATOR AT DARMSTADT \*)

V. Aab, K. Alrutz - Ziemssen, R. Amend, D. Flasche, H.-D. Gräf, V. Huck, K. D. Hummel,  
M. Knirsch, F. Lindqvist, W. Lotz, A. Richter, T. Rietdorf, U. Schaaf, S. Simrock,  
E. Spamer, A. Stiller, O. Titze, H. Weise, W. Ziegler  
Institut für Kernphysik, Technische Hochschule Darmstadt,  
Schlossgartenstr. 9, D - 6100 Darmstadt, Germany

and

H. Heinrichs, H. Piel, J. Pouryamout  
Fachbereich Physik, Universität Gesamthochschule Wuppertal,  
Gauss - Str. 20, D - 5600 Wuppertal, Germany

### Abstract

Since the superconducting injector linac of the accelerator produced a first beam in August 87 the first cryomodule of the main linac containing another two accelerating structures has been installed and operated. The final concept of the rf control circuits has been developed and two prototype channels were operated successfully in an acceleration test with five superconducting structures. The beam from the injector linac was used routinely for atomic and nuclear physics experiments during the last four months.

### I. Introduction

Reports on the status of the 130 MeV superconducting electron accelerator presently under construction at the Nuclear Physics Institute of the Technische Hochschule Darmstadt have been presented earlier [1,2] and the basic concept of the accelerator as well as its layout and principle of operation are treated in detail there. Therefore only the main design parameters (see Tab. I) are recalled here and a short description of the layout is given in Sect. II.

Table I: Design parameters of the accelerator

Beam energy / MeV		10 - 130
Energy spread / keV		$\pm 13$
cw current / $\mu\text{A}$		$\geq 20$
Operating frequency / MHz		2997
Number of structures	1.00 m long	10
Capture section	0.25 m long	1

Main emphasis is laid on the experience which could be gained in operating the three superconducting accelerating structures of the injector and the first two (out of eight) structures of the main linac and on the development of the final concept of the rf control circuits (covered in Sect. III) including the test of their first prototypes. Results from an acceleration test with five superconducting structures are discussed in Sect. IV while Sect. V contains a short summary of experiments (nuclear and atomic physics) using the beam from the superconducting injector. Finally in Sect. VI we give an outlook on how we intend to proceed in the completion of the accelerator and on some current investigations of possible improvements.

### II. Present Status

A schematic layout of the accelerator is shown in Fig. 1. The electron gun is followed by a 250 kV electrostatic preacceleration and the room temperature part of the injection where preformation of the bunches is accomplished. The superconducting injector linac uses a 5-cell capture section (0.25 m long) and two 20-cell accelerating structures (1 m long) to produce a 10 MeV beam. The main linac containing eight 20-cell structures increases the energy by 40 MeV and two beam transport systems each consisting of two isochronous  $180^\circ$  bends (like the injection into the main linac) and a straight section allow for two recirculations of the beam, increasing the energy to a maximum of 130 MeV.

\*) Work supported by Deutsche Forschungsgemeinschaft

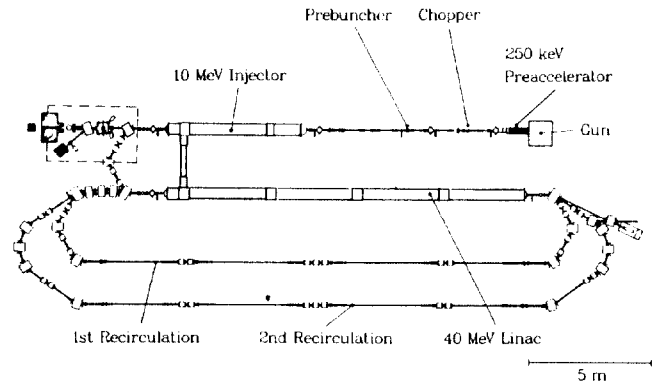


Fig. 1 Layout of the superconducting 130 MeV accelerator

Extraction of the beam to the experimental facilities for electron scattering is indicated in the extreme right portion of Fig. 1. The upper left portion shows two experimental setups, an apparatus for the investigation of channeling radiation and a facility for nuclear resonance fluorescence measurements (see Sect. V) in the straight beamline behind the injector linac.

The present status of installation is as follows: The room temperature part of the injector is in operation since some two years now. The beam transport systems for the injection and the two recirculations including the beamline and associated vacuum components are installed and ready for use. The superconducting injector linac is fully equipped with accelerating structures and has produced a first beam in August 87. The first of the four cryogenic modules of the main linac is equipped with two 20-cell structures and a beam accelerated by all five structures was obtained in May 88 (see Sect. IV). All rf transmitters (twelve klystrons, 500 W each) are installed and production of the rf control electronics (described in Sect. III) is in progress after a successful test of two prototypes establishing phaselocked operation of the main linac and the injector. The helium refrigerator and cryogenic components work very satisfactorily (they have been in operation for several periods of many weeks) but some shortcomings of the four stage roots pump, necessary for the 2 K operation, have still prevented a power and final acceptance test.

### III. RF Control System

To achieve phaselocked operation of several superconducting accelerating structures turned out to be the most time consuming task in the course of the construction of the accelerator. Careful investigations showed that mechanical vibrations, caused by the heavy machinery of the helium refrigerator (compressor and roots pumps) which are located close to the accelerator, are transmitted through the cryogenic transfer line into the cryostat and cause variations of the resonant frequencies of the superconducting structures. The sensitivity is extremely high, a change in length of  $1 \mu\text{m}$  of a 1 m long 20-cell structure results in a frequency shift of 500 Hz, and thus even a strongly overcoupled structure with a loaded quality factor of  $Q_L \approx 3 \cdot 10^7$  will show phase variations of  $\pm 0.45^\circ$  if its length is oscillating by as little as one nm! The original attempt to control the resonant frequency

of the structures mechanically by fast piezoelectric translators failed because of the mechanical resonances of the structures in the frequency range of 200 - 400 Hz, a fact that limits the use of the piezoelectric feedback control circuit to very low frequencies.

Therefore, in order to achieve the design value for the energy spread of the accelerated beam (see Tab. 1), an rf control system had to be developed that keeps phase variations (between any of the structures and the reference oscillator) below  $1^\circ$  and stabilizes the amplitude of the accelerating field to  $1 \cdot 10^{-4}$ . A first successful operation of the three structures in the injector linac was obtained using a concept very similar to the one described in [3] except that in our system the amplitude is controlled by a PIN attenuator and phase stabilization is achieved using a combination of a  $0^\circ$  power divider, two double balanced mixers (DBM), and a  $90^\circ$  hybrid acting as a power combiner. These modifications were necessary since a complex phasor modulator (CPM), the central control element used in the system of ref. [3], is not available for an operating frequency of 3 GHz. It seemed, however, disadvantageous, since precise digitally controlled phase shifters and attenuators at 3 GHz are very expensive, to use this concept for the twelve rf channels required for the operation of the complete accelerator where computer control of the system is a necessity.

Thus, we decided to use the principle of ref. [4] where a minimum of rf elements is used and where all control functions are performed at low frequencies. Operation of the system can be deduced from Fig. 2 which shows a simplified block diagram. The accelerating structure (cavity) driven by the klystron is part of a self excited loop. A monitor signal from the structure is downconverted in an rf vector demodulator (bottom left of Fig. 2). The two output signals from the demodulator represent orthogonal components of a vector describing the field of the accelerating structure in the frame of the reference oscillator, thus containing complete information about amplitude and phase. These signals travel through the low frequency (IF) part of the control circuitry (right portion of Fig. 2) before they are upconverted in frequency by an rf vector modulator (top left of Fig. 2). The output of this modulator is amplified by the klystron, closing the self excited loop.

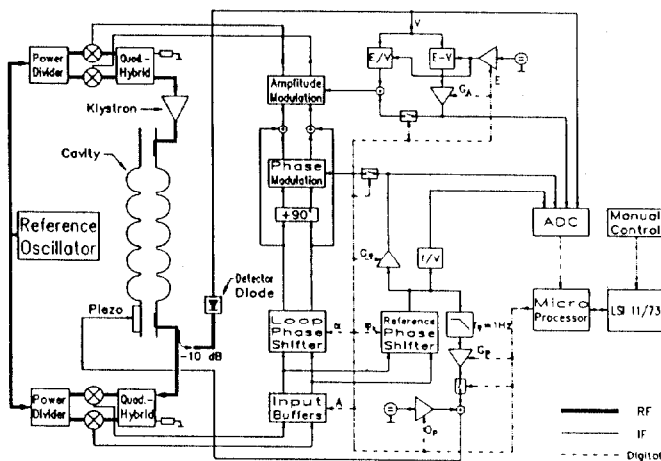


Fig. 2 Simplified block diagram of the rf control circuit

In the IF section the signals pass through variable gain input buffer amplifiers, a rotational matrix acting as a loop phase shifter, a phase controller which is a low frequency CPM, and analog multipliers used for amplitude control. The amplitude error signal is derived by comparing an internal reference  $E$  (top right of Fig. 2) with a signal obtained from a Schottky-detector diode. In this circuit the limiting function  $E/V$  is always active while the actual feedback control with gain  $G_A$  is switchable. The phase error signal is obtained by passing the signals from the input buffers through another rotational matrix, the reference phase shifter. It is then amplified ( $G_p$ ) and can be switched to the phase modulator to obtain phase control. The low frequency components of the output from the reference phase shifter are used (bottom right of Fig. 2) to correct slow frequency shifts of the accelerating structures through the piezoelectric translators.

The single board microcomputer used to control the rf channels is a development of our laboratory, based on an MC 68020 processor. Through an analog data acquisition (ADC) it is able to keep track of the most important analog signals in the IF section (some of them indicated in Fig. 2). Not shown in Fig. 2 is an analog bus which allows to switch nine analog signals to cable drivers from where they are transmitted to an oscilloscope in the control room.

The consequent separation of microwave and low frequency components in this concept led to a very space and cost effective solution: All rf parts except for a small external 20 dBm amplifier could be integrated onto a single stripline printed circuit board taking only one slot of a NIM crate. By using new LSI circuits also the IF section could be realized on a single board in a VME Bus crate which also contains the microcomputer and the analog bus drivers.

Two prototypes of this control circuitry have been tested successfully establishing phaselocked operation between the two accelerating structures of the main linac and the injector. The left photograph of Fig. 3 shows a polar presentation of the output signals from the rf vector demodulator on an oscilloscope, the dots representing the tip of the rf field vector in the frame of the reference oscillator. For this picture the reference phase has been stepped in increments of  $10^\circ$  at a speed of 30 ms/step. Traces between the  $10^\circ$  steps in some portions of the picture are due to overshoot in the feedback control caused by nonlinearities still present in the rf vector modulator. They are however caused by the stepping of the reference phase and disappear when a steady state is controlled. In that case only a single spot is visible and a change of the reference phase by  $1^\circ$  can be distinguished clearly. For such a steady state condition the right photograph of Fig. 3 shows the output signals from the IF section in the same polar presentation, giving an impression of how much correction in the radial (amplitude control) as well as in the tangential (phase control) direction is needed to keep the field in the structure stable in amplitude and phase.

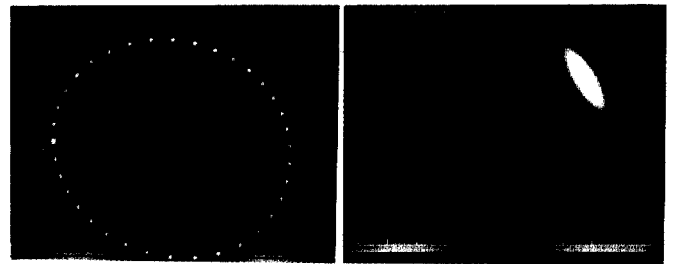


Fig. 3 Output signals of the rf vector demodulator (left) in polar presentation. The reference phase is stepped in increments of  $10^\circ$ . Input signals to the rf vector modulator (right) for a single setting of the reference phase, same presentation.

The two photographs in Fig. 4 show a phase error signal (left) as obtained from an independent DBM and the amplitude signal (right) from the Schottky-detector diode in time representation.

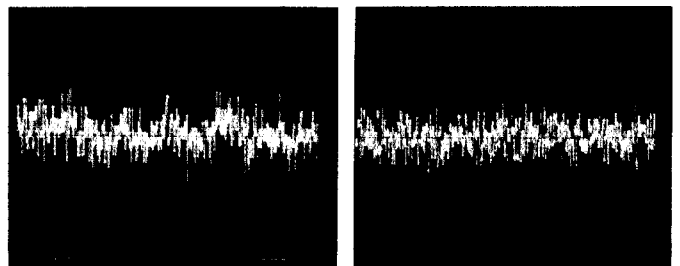


Fig. 4 Phase error signal in time representation (left). Sensitivities are 1 mV/div corresponding to  $0.2^\circ$ /div vertically and 5 ms/div horizontally. AC components of amplitude signal from the Schottky-detector diode (right). Sensitivities are 2 mV/div vertically and 5 ms/div horizontally. The DC level amounts to 1400 mV.

The signals show that phase variations amount to less than  $\pm 0.3^\circ$  and that the amplitude was controlled to within  $\pm 3 \cdot 10^{-3}$ . It should be noted that most of the "noise" dominating the signals in Fig. 4 is due to pickup from the power supplies of the klystrons at present limiting the performance of the feedback control circuits, a situation which certainly can be improved in the near future.

#### IV. Beam Tests

A first beam test with the injector linac [2] produced a beam of 6.8 MeV from which accelerating fields of 6 MV/m for the capture section (#1), 3.2 MV/m for the first (#2), and 2.5 MV/m for the second (#3) 20-cell structure could be inferred. The limiting effects were electron loading for the two structures (#1 and #3) fabricated from niobium of medium purity (RRR  $\approx 100$ ) and a thermal quench for #2 which is made out of reactor grade niobium. Several attempts of helium processing raised the maximum field of #3 to 4.2 MV/m still limited by electron loading but did not affect the fields of #1 and #2. This however raised the maximum beam energy of the injector linac to 8.5 MeV. It seems that further improvement can only be achieved by either replacing or at least rinsing the structures with ultrapure water.

The first two structures (#4 and #5) of the main linac both fabricated from reactor grade niobium showed after their installation fields of 3 MV/m and 1 MV/m, respectively. Extensive helium processing did not affect #4 but brought the field of #5 up to 3 MV/m. In the meantime this number has come down to 1 MV/m again (#5) and #4 shows frequency instabilities which prevent a phaselocked operation at fields in excess of 1 MV/m. This is very likely due to the adsorption of nitrogen because of a small leak in the vacuum system of the beam line.

Nevertheless when the two prototypes of the new rf control circuits had become operational they were used to control the fields of structures #4 and #5 and to obtain phaselocked operation with the three structures of the injector linac. An 8 MeV beam from the injector was transported around the  $180^\circ$  isochronous bend and through the first module of the main linac. Behind this module a viewscreen and a thick target for bremsstrahl production had been installed. The beam diameter could be kept

within a few millimeters in front of and behind the module without any intermediate focusing. Using a NaI detector bremsstrahl spectra at  $0^\circ$  were taken. Four such spectra are displayed in Fig. 5. An endpoint energy of 8 MeV was obtained from the injector beam with no field in structures #4 and #5. Adding #5 and #4 to the acceleration process increased the endpoint energy to 9.2 and 10 MeV respectively, indicating a field of about 1 MV/m for both structures. As mentioned above the field in structure #4 could be increased if the phase control circuit was switched off, the fourth spectrum in Fig. 5 with an endpoint energy of 12 MeV was obtained under this condition, which of course produces a beam with a huge energy spread.

Despite the very disappointing fields of structures #4 and #5 we will leave them installed. A warm up to room temperature which is necessary anyway for the installation of the next cryo-module of the main linac will remove the adsorbed nitrogen and after repair of the leak in the beamline another attempt of helium processing will be made during the next test period.

#### V. Experiments

During the last four months the beam from the superconducting injector was used quite extensively (mostly during night hours) for the two experiments installed at the end of the straight beam line (see Fig. 1, top left). A summary of beam energies, currents, and time used for these experiments is given in Tab. 2.

Table 2: Experimental use of the injector linac

Experiment	Energy / MeV	Current / $\mu$ A	Time / h
Channeling Radiation	3.9 - 7.7	0.01	80
Nucl. Resonance Fluorescence	2.5 - 8.5	30	260

The channeling radiation experiment [5] required rather low currents on the order of 10 nA but the best beam quality obtainable since the Si(Li) detector was positioned at  $0^\circ$  behind the crystal target and the electron beam from the accelerator was neither deflected by a beam transport system nor collimated before hitting the target. In Fig. 6 a typical channeling radiation spectrum is shown, obtained from a  $10 \mu\text{m}$  thick silicon crystal target in the  $\langle 111 \rangle$  orientation. A data taking time of 4 minutes was sufficient to observe the four channeling radiation lines labelled in the standard notation [6]. Background has been eliminated by measuring and subtracting a bremsstrahl spectrum under identical conditions but with the orientation of the crystal changed by a few degrees.

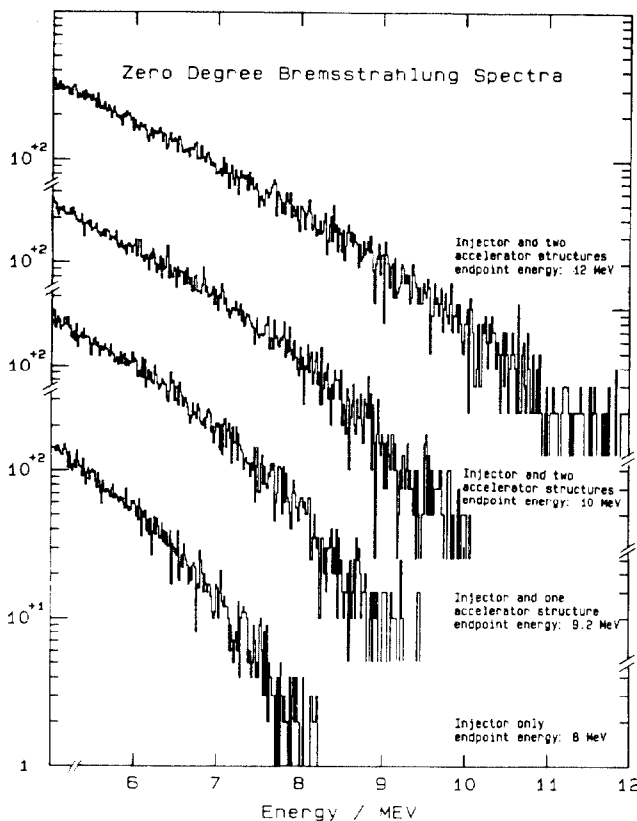


Fig. 5 Bremsstrahl spectra measured with a NaI detector behind the first module of the main linac.

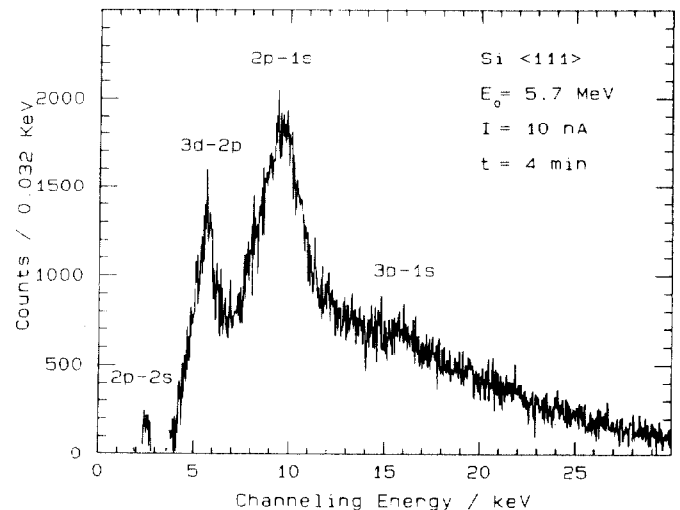


Fig. 6 Measurement of channeling radiation, using the injector beam. Lines are labelled according to ref. [6].

The nuclear resonance fluorescence experiment required high currents because of the small cross sections involved, most of the time 30  $\mu$ A were used. Without any focusing elements behind the injector linac the spot size at the exit window (about 5 m downstream the beamline) was only 4-5 mm in diameter. A typical spectrum (no background has been subtracted) obtained by irradiating a  $^{154}\text{Sm} - ^{27}\text{Al}$  sandwich target with a 4.6 MeV bremsstrahlung spectrum is shown in Fig. 7. Indicated are the 2.98 MeV calibration line from  $^{27}\text{Al}$  and the line corresponding to the M1 transition from the 3.193 MeV state in  $^{154}\text{Sm}$  as found by inelastic electron scattering [7]. The spectrum also shows inelastic transitions (indicated by arrows) to the first  $2^+$  state in  $^{154}\text{Sm}$ , about 82 keV below the elastic transitions.

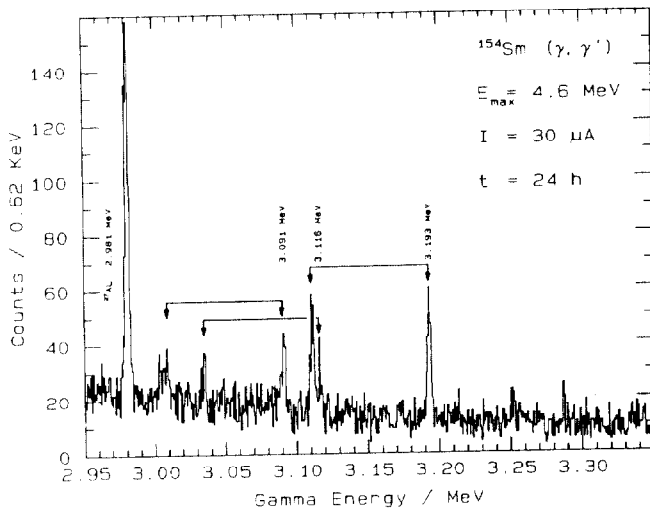


Fig. 7 Spectrum from a nuclear resonance fluorescence experiment, performed at the end of the injector beam line. For details see Sect. V of text.

## VI. Outlook

Presently the accelerator cryostat is warmed up to room temperature for the installation of the second module of the main linac, equipped with another two 20-cell structures. By increasing the number of superconducting structures in operation the information on their average performance will become more reliable. This is very important since most of our accelerating structures have been fabricated some four years ago from reactor grade niobium and if they will not show reasonable field strengths they have to be replaced by new ones made from high purity material.

The new rf control circuitry (described in Sect. III) is in production for all twelve rf channels needed for the operation of the complete accelerator. As soon as the accelerator will produce a beam with an energy of at least 20 MeV a first attempt to recirculate and to accelerate it a second time will be made.

Parallel to the accelerator development a study [8] has been performed investigating the possible operation of a Free-Electron-Laser (FEL) in a bypass of the first recirculation. The very promising results of this study and the proposed realization of this project are presented in a separate contribution [9] to this conference.

## Acknowledgement

We are very much indebted to I. Ben-Zvi for his essential help during his visit in Darmstadt. The support from H. Lengeler and E. Haebel by fruitful discussions and help with equipment is gratefully acknowledged. We thank G. Sprouse for providing us with important information and his encouragement. Stimulating discussions with D. Proch, K. Shepard and A. Schwefman have been very helpful in the course of the project. We are very grateful for the enormous help provided by the technical staff at the DALINAC and the mechanical and electronics workshops of both respective Institutions.

## References

- [1] K. Alrutz - Ziemssen, H.-D. Gräf, V. Huck, K. D. Hummel, G. Kaster, M. Knirsch, A. Richter, M. Schanz, S. Simrock, E. Spamer, O. Titze, T. Grundey, H. Heinrichs, H. Piel, Proc. 1986 Lin. Acc. Conf., SLAC 303, Stanford, Cal. USA (1986) 512.
- [2] V. Aab, K. Alrutz - Ziemssen, R. Arnend, D. Flasche, H.-D. Gräf, V. Huck, K. D. Hummel, M. Knirsch, W. Lotz, A. Richter, T. Rietdorf, U. Schaaf, S. Simrock, E. Spamer, O. Titze, H. Weise, W. Ziegler, H. Heinrichs, H. Piel, J. Pouryamout, Proc. Third Worksh. on RF Supercond., ANL-PHY-88-1, Argonne, Ill. USA (1988) 127.
- [3] I. Ben - Zvi, M. Birk, C. Broude, G. Gitliz, M. Sidi, J. S. Sokolowski, J. M. Brennan, Nucl. Instr. A 245 (1986) 1.
- [4] J. R. Delayen, G. J. Dick, J. E. Mercereau, IEEE Trans. Nucl. Sci. NS-24, No. 3 (1977) 1759.
- [5] W. Lotz, H. Genz, A. Richter, W. Knüpfer, J. P. F. Sellschop, J. Physique, C 9, (1987) 95.
- [6] J. U. Anderson, E. Bonderup, R. H. Pantell, Ann. Rev. Nucl. Part. Sci., 33, (1983) 453.
- [7] D. Bohle, G. Kuchler, A. Richter, W. Steffen, Phys. Lett. 148B (1984) 260.
- [8] V. Aab, K. Alrutz - Ziemssen, H.-D. Gräf, A. Richter, A. Gaupp, Proc. 9<sup>th</sup> Int. FEL Conf., Sept. 14-18, 1987, Williamsburg, Va., USA (to be published).
- [9] V. Aab, K. Alrutz - Ziemssen, H. Genz, H.-D. Gräf, A. Richter, H. Weise, A. Gaupp, Proc. 1988 Europ. Part. Acc. Conf., June 7-11, 1988, Rome, Italy (to be published).